Available online at www.sciencedirect.com
SCIENCE DIRECT®
Journal of Chromatography B, 790 (2003) 161–173
JOURNAL OF CHROMATOGRAPHY B
www.elsevier.com/locate/chromb

# Whey proteins as a model system for chromatographic separation of proteins

Linda Pedersen[a], Jørgen Mollerup[a,*], Ernst Hansen[a], Alois Jungbauer[b]

[a]*Engineering Research Centre IVC-SEP, Department of Chemical Engineering, Technical University of Denmark, Building 229, DK-2800 Lyngby, Denmark*
[b]*Institute for Applied Microbiology, University of Agriculture and Forestry and Biotechnology, Vienna, Austria*

**Abstract**

Although chromatographic separation of whey proteins has been considered too expensive, whey may serve as an excellent model mixture to investigate and validate the use of simulation tools in the development and optimization of chromatographic separations and the outcome could easily be utilized since the model system has an intrinsic value. Besides, milk from transgenic animals could be an attractive source of pharmaceuticals which must be separated from the other proteins in the milk. Several whey proteins are of interest especially, α-lactalbumin, β-lactoglobulins, immunoglobulins, lactoperoxidase, and lactoferrin. The scope of the project is to develop a consistent set of chromatographic data for whey proteins including isotherms, transport properties and scale-up studies and to develop the appropriate models for the anion exchangers Q-Sepharose XL, Source 30Q, Ceramic Q-HyperD F, and Merck Fractogel EMD TMAE 650 (S). In this work we have determined and correlated gradient and isocratic retention volumes in the linear range of the isotherm for α-lactalbumin, β-lactoglobulin A and B, and bovine serum albumin at a pH from 6 to 9 at various NaCl concentrations.


*Keywords:* Anion exchangers; Mathematical modelling; Gradient elution; Steric mass action; Proteins; Whey proteins; Lactalbumin; Lactoglobulin; Albumin

## 1. Introduction

Preparative chromatographic separation techniques are of singular importance to the biopharmaceutical industry because they can deliver high-purity products, are relatively easy to develop, and can readily be scaled from the laboratory scale to the desired production level [1]. Hence, one reason for the ubiquity of chromatographic steps in preparative protein purification is that they provide a relatively efficient means to meet manufacturing goals of the biopharmaceutical industry. However, though easy to develop, they are complex processes to optimize because of the very many process parameters such as choice of media, salt, buffer, organic solvent, temperature, gradient, etc. The importance of this unit operation therefore accounts for the attention focused on a greater understanding of the chromatographic separation through a combination of laboratory investigations and modelling. Whey proteins may thus serve as an excellent model mixture to investigate the use of simulation tools in the development and optimization of chromatographic separations. The composition of major proteins in bovine whey is shown in Table 1.

Hahn et al. [2] investigated a fractionation scheme

*Corresponding author. Tel.: +45-4-525-2866; fax: +45-4-588-2258.
*E-mail address:* jm@kt.dtu.dk (J. Mollerup).

1570-0232/03/$ – see front matter 
doi:10.1016/S1570-0232(03)00127-2

Table 1
Major protein composition in bovine whey

| | Concentration (g/l) | Isoelectric point (p*I*) | $M_r$ |
|---|---|---|---|
| β-Lactoglobulins | 3–4 | 5.2–5.4 | 18 300 |
| α-Lactalbumin | 1.2–1.5 | 4.7–5.1 | 14 200 |
| Serum albumin | 0.3–0.6 | 4.9–5.1 | 66 000 |
| IgG, IgA, IgM | 0.6–0.9 | 5.8–7.3 | 150 000–900 000 |
| Lactoperoxidase | −0.06 | 9.6 | 78 000 |
| Lactoferrin | −0.05 | 8.0 | 78 000 |

From Ref. [2].

for IgG, lactoferrin and lactoperoxidase based on the cation exchangers S-HyperD F, S Sepharose FF, Fractogel EMD-S 650 (S) and Macro-Prep High S. They investigated the binding capacities for IgG and the different elution behaviours when sequential step gradients with NaCl buffers were applied. Strange et al. [3] review the analytical and preparative methods of whey proteins developed prior to 1992. Konecny et al. [4] used thiophilic chromatography on a T-gel to purify IgG from sweet cheese whey and found this method suitable for large-scale whey IgG isolation. Jen and Pinto [5] investigated the chromatographic retention and peak shape of β-lactoglobulins A and B for various nonlinear chromatographic modes of operation including isocratic and gradient elution and frontal and displacement chromatography on a PAE-300 ion exchanger. Colby et al. [6] investigated the effect of compression on the scale-up of a commercial packed-bed ion-exchange process to manufacture a whey growth factor extract using lactoperoxidase and lactoferrin as model substances. Vogt and Freitag [7] investigated the suitability of anion-exchange and hydroxyapatite displacement chromatography for the processing of technical dairy whey. Gerberding and Byers [8] described a preparative ion-exchange chromatographic process for the separation and recovery of the four major proteins [α-lactalbumin, β-lactoglobulin, bovine serum albumin (BSA) and IgG] and lactose from sweet dairy whey. In that work, it was found that the anion-exchange step was most effective in separating β-lactoglobulin from the feed mixture while a cation-exchange step was used to further recover the IgG. Walash and Nam [9] have developed an affinity enrichment process of bovine lactoferrin of whey, and recently Lan et al. [10] used a liquid–solid circulating fluidized bed ion-exchange extraction system for continuous protein recovery from cheese whey.

In this work we have determined and correlated gradient and isocratic retention volumes in the linear range of the isotherm for α-lactalbumin, β-lactoglobulin A and B, and BSA at pH values from 6 to 9 at various NaCl concentrations on the anion exchangers Q-Sepharose XL, Source 30Q, Merck Fractogel EMD TMAE 650 (S) and Ceramic Q-HyperD F. A model for simultaneous correlation of the isocratic and gradient elution data are presented. An integral part of this model is the model for the distribution ratio in the linear range which shall be obtained from a nonlinear isotherm model as the limit of the distribution ratio at zero protein concentration. The model for the isotherm shall be extendable to multicomponent systems in a consistent manner. The steric mass action (SMA) formalism developed by Brooks and Cramer [11] fulfils these conditions. It is a three-parameter model where the distribution ratios in the linear range determine two of the three parameters in the model. The third parameter in the SMA formalism, the steric hindrance factor, can be determined from a few capacity measurements.

Other retention models [12–16] have been investigated but none of these models were able to correlate the experimental data with the same precision as the SMA formalism. The Langmuir isotherm is widely used for correlation of adsorption behaviour, Guiochon et al. [17], but it is not suited in the linear range because the dependence of the distribution ratio on the salt concentration cannot be derived from the model. Besides, the extension of the Langmuir isotherm to multicomponent systems is not straightforward because the maximum adsorption capacity

must be the same for all solutes or the result is not thermodynamically consistent [18].

## 2. Experimental

### 2.1. Chromatographic media

The media used were: Source 30Q (lot No. 242339) and Q Sepharose XL (lot No. 245698) from Amersham Biotech and Ceramic Q-HyperD F (lot No. 8088) from BioSepra. The Merck Fractogel EMD TMAE 650 (S) was a prepacked 50–10 cartridge, catalogue No. 20338. The particle diameters of the media, the column dimensions, and the estimated column capacities are shown in Table 2. The particle diameters are those stated in the information material enclosed with the media.

### 2.2. Chemicals

BSA (A-6918) purity 98%, α-lactalbumin (L-5385) purity 85%, β-lactoglobulin A and B (L-0130) purity 90%, β-lactoglobulin A (L-7880) purity 90%, β-lactoglobulin B (L-8005) purity 90%, Bis-Tris propane (B-6755) were all from Sigma (St. Louis, MO, USA). The purity is according to the manufacturer. 5 *M* NaCl (1.06404.1000) and 5 *M* $NaNO_3$ (1.06537.1000) were from Merck (Darmstadt, Germany). HCl (LAB00440) and NaOH (LAB00334) were from Bie and Berntsen (Denmark). Standard solutions for calibration of the pH meter at pH 4.005, 7.000, and 10.012 were from Radiometer (Denmark).

### 2.3. Equipment

The BioCAD Chromatographic Workstation is from Perseptive Biosystems (Cambridge, MA, USA). The eluting peaks were detected at 280 nm. The pH meter (pHM 92) was from Radiometer. The 0.22-μm filters were from Millipore. One prepacked column Fractogel EMD TMAE 650(s) (article No. 20338) was from Merck. The other columns were packed in HR10/10 and HR16/10 columns from Amersham Biotech (Uppsala, Sweden).

### 2.4. Sample preparation

Two stock solutions were prepared at each pH, i.e. 6, 7, 8 and 9. The first solution was prepared by dissolving 20 m*M* Bis-Tris propane in pure water and adding 5 *M* HCl to reach the desired pH value. The second solution was prepared by dissolving 20 m*M* Bis-Tris propane in a 1.0 *M* NaCl solution and adding 5 *M* HCl to reach the same pH value as the first solution. All the other buffers were prepared by mixing of the two stock solutions followed by an addition of 5 *M* HCl or 5 *M* NaOH to the same pH as the stock solutions. Independent solutions of each one of the proteins under study were prepared by dissolving 3 g/l in an appropriate buffer solution. For some of the experiments a solution of the mixture of β-lactoglobulin A and B (L-0130) was used. All solutions were filtered through 0.22-μm filters. The pH meter was calibrated with two standard solutions at pH 4.005 and 7.000 or 7.000 and 10.012.

### 2.5. Linear gradient elution

The gradient elution was preformed at gradient volumes of 16, 32, 64, 128 and 256 ml using two buffer solutions at about 20–40 m*M* NaCl and 250 m*M* or 350 m*M* NaCl, respectively. The flow-rate was 6 ml/min. The injected protein solutions were prepared by dissolving 3 g protein/l in the starting

Table 2
Investigated media and column dimensions

| | Particle diameter (μm) | Column volume (ml) | Column diameter (mm) | Column capacity (mequiv.) |
|---|---|---|---|---|
| Source 30Q | 30±3 | 8.1 | 10 | 0.843 |
| Ceramic Q-HyperD F | 50±15 | 7.6 | 10 | 2.384 |
| Merck Fractogel 650 | 20–40 | 3.9 | 10 | 0.112 |
| Q-Sepharose XL | 45–165 | 7.6 | 16 | 2.154 |

buffer solution. The column was equilibrated with 40 ml of the starting buffer and the UV detector was zeroed. A 100-μl volume of the protein solution was loaded and the gradient and the data collection started. At the end of the gradient 40 ml of buffer was passed through the column to ensure that all the protein was eluted. Finally the column was regenerated with a 1 *M* NaCl solution.

### 2.6. Isocratic elution

The column was equilibrated with 40 ml of buffer and the UV detector was zeroed. The column was loaded with 100 μl of a sample solution containing 3 g protein/l and the data collection and the elution started. The salt concentrations used varied from 40 m*M* to 1 *M*. The lower limit depends on the binding strength of the protein. When the retention volume was in the order of 10 times the column volume the response curve was so flat that it was useless. At the end of the elution the column was regenerated with a 1 *M* NaCl solution. The retention volume of the proteins was also determined using a 1 *M* NaCl buffer (nonbinding conditions). The flow-rates were 1, 3 and 6 ml/min. The salt retention volume was determined by injecting a small pulse of a diluted nitrate solution onto the column using a 1 *M* sodium nitrate buffer.

### 2.7. Estimation of the dead volumes

The dead volume from the injection to the detector was determined by injecting a small pulse of $NaNO_3$ solution without a column inserted by joining the tubes together. The dead volumes in the tubing, distributers and filters in the HR 10/10 and the HR16/10 columns were determined by inserting an empty column with the distributers pressed close together. In order to determine the dead volume from the mixer to the detector the column was removed the tubes joined together and the system filled with a $NaNO_3$ solution. The dead volume was determined by displacing the nitrate solution with water.

The salt displacement volume from the mixer to the detector is equal to the dead volume from the mixer to the detector plus the true salt retention volume in the column and the dead volume in the tubing, distributers and filters on the column.

### 2.8. Determination of the retention volume

The retention volume was determined from the centre of mass of the eluting peak by fitting the response curve to the exponential modified Gauss (EMG) function. Some of the peaks from the elution of the β-lactoglobulin A and B mixture could not be fitted due to insufficient peak separation. therefore the retention volumes were taken to be the peak maxima. The true retention volume of a solute equals the measured retention volume minus the dead volume from the injection to the detector including the dead volume in the column tubing, distributers and filters.

### 2.9. Steric mass action formalism

The SMA formalism by Brooks and Cramer [11] is a three-parameter model for multicomponent protein–salt equilibria. The protein is bound to the stationary phase at a number of exchange sites given by an effective charge $z_p$ which most often is less than the net charge of the protein because not all charges on the protein surface can be attached to the ligands. The equilibrium constant for an ion-exchange process is defined as

$$K = \left(\frac{q}{c}\right) \cdot \left(\frac{c_{salt}}{q_{salt}}\right)^{\nu} \quad (1)$$

where $\nu = z_p/z_s$ is a charge ratio, $z_p$ is the effective charge of the protein, and $z_s$ is the charge of the counterion from the salt, $c$ is the protein concentration in the mobile phase, $q$ is the protein concentration in the adsorbed state in the gel, $c_{salt}$ is the counterion concentration in the mobile phase and $q_{salt}$ is the counterion concentration in the adsorbed state in the gel. The effective charge of the protein depends on the pH. Brooks and Cramer [11] assumed ideal solution behaviour therefore activities could be replaced by concentrations. The large protein molecule sterically shields a number of sites that will be unavailable for exchange therefore Brooks and Cramer [11] introduced a steric hindrance factor $\zeta$ where $\zeta q$ is the number of co-ion charges on the resin unavailable for exchange due to the size of the protein. The hindrance factor depends on the size and the conformation of the protein molecule. Electroneutrality requires that the sum of

the positive and negative charges in the exchanger is zero. If the capacity (equiv./l pore volume) of the ion exchanger is $\Lambda$, electroneutrality requires that

$$\Lambda = z_s q_{salt} + (\zeta + z_p)q \quad (2)$$

Inserting $q_{salt}$ from Eq. (2) in Eq. (1) gives

$$K = \left(\frac{q}{c}\right) \cdot \left[\frac{z_s c_{salt}}{\Lambda - (\zeta + z_p)q}\right]^{\nu} \quad (3)$$

Using standard thermodynamics, the equilibrium constant $K$ can be calculated from the standard Gibbs energy changes [19]

$$RT \ln K = -\Delta G^0_{protein} + \nu \Delta G^0_{counterion} \quad (4)$$

where $\Delta$ is the difference between $G^0$ in the adsorbed state and the solute state. In the linear range of the isotherm, where $\Lambda > (\zeta + z_p)q$, because $q$ is very small, we can make the approximation that

$$K = \left(\frac{q}{c}\right) \cdot \left(\frac{z_s c_{salt}}{\Lambda}\right)^{\nu} \quad (5)$$

We solve for $q/c$ and define this ratio as the distribution ratio $A$ in the linear range

$$A = \frac{q}{c} = K \cdot \left(\frac{\Lambda}{z_s c_{salt}}\right)^{\nu} \quad (6)$$

Eqs. (4) and (6) comprise the model we use to correlate the distribution ratio $A$ at low protein concentrations where the isotherm becomes linear.

### 2.10. Isocratic elution

In linear chromatography the retention volume is calculable from the velocity of the centre of mass of the eluting peak. This velocity depends on the void fractions in the column and in the particle and the distribution ratio $A$. The interstitial porosity $\varepsilon$ is the fractional void volume between the particles and the intraparticle porosity $\varepsilon_p$ is the fractional void volume in the particle. The fractional void volume in the particle available for a molecule is $\varepsilon_p K_d$ where $K_d$ is an exclusion factor which per definition is 1 for the salt and less than 1 for large molecules like proteins. The result is

$$V_R = V_{column}[\epsilon + (1 - \epsilon)\epsilon_p K_d(1 + A)] \quad (7)$$

where $V_{column}$ is the column volume. This equation is formally derived from the material balance provided that mass transfer effects can be neglected. Further details are given elsewhere [20]. The retention volume of a nonadsorbed species is the retention volume when $A = 0$

$$V_{NA} = V_{column}[\epsilon + (1 - \epsilon)\epsilon_p K_d] = V_{column}\epsilon_t \quad (8)$$

where $\varepsilon_t$ is the total column porosity; $\varepsilon_t$ depends on the size of a molecule, it equals the interstitial porosity $\varepsilon$ for a totally excluded molecule $K_d = 0$ and attains its largest value for a salt where $K_d = 1$. Inserting the Eqs. (6) and (8) in Eq. (7) gives the result

$$V_R = V_{NA} + V_{column}(1 - \epsilon)\epsilon_p K_d K \cdot \left(\frac{\Lambda}{z_s c_{salt}}\right)^{\nu} = V_{NA} + B \cdot \left(\frac{\Lambda}{z_s c_{salt}}\right)^{\nu} \quad (9)$$

where the equilibrium constant $K$ can be correlated by Eq. (4) and $B$ is

$$B = V_{column}(1 - \epsilon)\epsilon_p K_d K \quad (10)$$

Note that Eq. (9) implies that a plot of the log $(V_R - V_{NA})$ versus the log $(c_{salt})$ yields a straight line with a slope of $-v$. For proteins, $V_{NA}$ is determined as the retention volume in a 1–2 $M$ salt buffer.

### 2.11. Linear gradient elution

The gradient parameter $G$ is defined as

$$G = \frac{c_{salt_1} - c_{salt_0}}{V_g} \quad (11)$$

where $V_g$ is the gradient volume and $c_{salt_0}$ and $c_{salt_1}$ are the initial and the final salt concentrations of the gradient. Because the gradient is linear the adsorbate elutes at a salt concentration, $c_{salt}$, determined by the gradient parameter $G$

$$G = \frac{c_{salt_1} - c_{salt_0}}{V_g} = \frac{c_{salt_1} - c_{salt_0}}{V_{R_g} - V_{R_{salt}}} \Rightarrow$$

$$c_{salt} = c_{salt_0} + G(V_{R_g} - V_{R_{salt}}) \quad (12)$$

where the salt retention volume is calculable from Eq. (8) with $K_d = 1$. Yamamoto et al. [20] have derived the formula for the eluting salt concentration

$c_{salt}$ using a model similar to the SMA formalism in the linear range. When $A \gg 1/K_d - 1$ the result is

$$\int_{c_{salt_0}}^{c_{salt}} = c_{salt}^{\nu} dc_{salt} = \frac{GB}{L} \cdot \left(\frac{A}{z_{salt}}\right)^{\nu} \int_0^L dz \quad (13)$$

where $B$ is a composite parameter defined in Eq. (10). Performing the integration gives the result

$$c_{salt} = \left[ GB\left(\frac{\Lambda}{z_s}\right)^{\nu} \cdot (\nu + 1) + c_{salt_0}^{\nu+1} \right]^{\frac{1}{\nu+1}} \quad (14)$$

Combining the Eqs. (12) and (14) gives the desired result for the retention volume at linear gradient elution

$$V_{R_s} = V_{R_{salt}} + \frac{1}{G} \cdot \left[ GB \cdot \left(\frac{\Lambda}{z_s}\right)^{\nu} \cdot (\nu + 1) + c_{salt_0}^{\nu+1} \right]^{\frac{1}{\nu+1}} - \frac{c_{salt_0}}{G} \quad (15)$$

Comparing the formula for the isocratic retention volume (9) to the above formula for the retention volume at linear gradient elution shows that we can correlate the two elution modes using the same model parameters, that is $B$, $\nu$ and $\Lambda$ provided $G$ is specified.

### *2.12. Estimation of model parameters*

The parameters we have to determine are the interstitial porosity $\varepsilon$, the intraparticle porosity $\varepsilon_p$, the exclusion factor $K_d$, the capacity $\Lambda$, the standard Gibbs energy changes $\Delta G^0_{protein}$ and $\Delta G^0_{counterion}$ and the charge ratio $\nu$. The parameters $\varepsilon$, $\varepsilon_p$, $\Lambda$, and $\Delta G^0_{counterion}$ are specific for the media although $\varepsilon$ varies with the quality of the column packing due to bed compaction. $K_d$ and $\Delta G^0_{protein}$ values depend on the protein and the media. $\Delta G^0_{protein}$ is assumed to be independent of the pH. The charge ratio $\nu$ depends on the media, the protein, and the pH.

The value of $\varepsilon + (1-\varepsilon)\varepsilon_p$ was determined from the nitrate retention volume in a 1 $M$ sodium nitrate buffer. Previously [21] we have used blue dextran ($M_r = 2\,000\,000$) and dextran conjugate ($M_r = 8\,000\,000$) to estimate the porosity $\varepsilon$ in different columns packed with S-HyperD and some other cation-exchange media but the results obtained on anion-exchange media were not satisfactory, probably due to some unspecific binding. It was therefore decided to assess a reasonable value for $\varepsilon$ similar to those obtained from the cation-exchange media or published data and calculate $\varepsilon_p$ from the measured retention volume of the salt. Within reasonable limits the results of the correlation of the data is not sensitive to the choice of $\varepsilon$.

The exclusion factor $K_d$ was determined from the retention volume of the protein in a 1 $M$ NaCl buffer using Eq. (8). The capacity $\Lambda$ was determined as the number of nitrate equivalents per litre of pore volume. $\Delta G^0_{protein}$, $\Delta G^0_{counterion}$, and $\nu$ were determined by a least square fit of the distribution ratio $A$ to the model, Eqs. (4) and (6). The distribution ratio $A$ was determined from the isocratic elution volume using Eq. (7).

## 3. Results and discussion

### *3.1. Comparison of experimental and calculated results*

The results are shown in Figs. 1–8. For a given chromatographic media, each figure shows the retention behaviour of the four whey proteins at one value of pH. Each figure has two graphs. The upper graph shows a comparison of the experimental and correlated isocratic retention volumes of four whey proteins in dependence of the salt (chloride ion) concentration of the eluting buffer. The retention volumes were correlated using the Eqs. (4) and (9). The apparent scatter in the experimental data was due to the observable fact that an increase in the flow-rate decreased the retention volume slightly. The lower graph shows a comparison of the experimental and calculated salt (chloride ion) concentrations at which the proteins elute in the gradient elution mode. We cannot compare the experimental gradient retention volumes for the different proteins because the initial and the final salt concentrations, $c_{salt_0}$ and $c_{salt_1}$, used for the four proteins differ depending upon how strong the protein binds. The experimental value of the salt concentration $c_{salt}$ at which a protein elutes was calculated from the

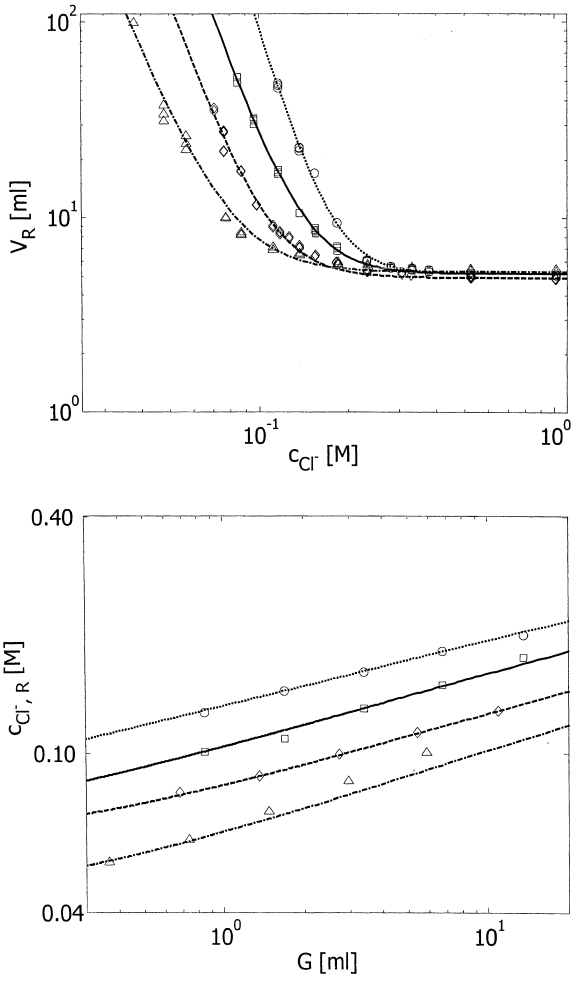


Fig. 1. Whey proteins on Source 30Q at pH 6. Comparison of experimental and correlated isocratic retention volumes (top) and experimental and predicted chloride ion concentrations at gradient elution (bottom). BSA: ◇, exp., - - -, model; α-lactalbumin: △, exp., –·–, model; β-lactoglobulin A: ○, exp., ····, model; β-lactoglobulin B: □, exp., —, model.

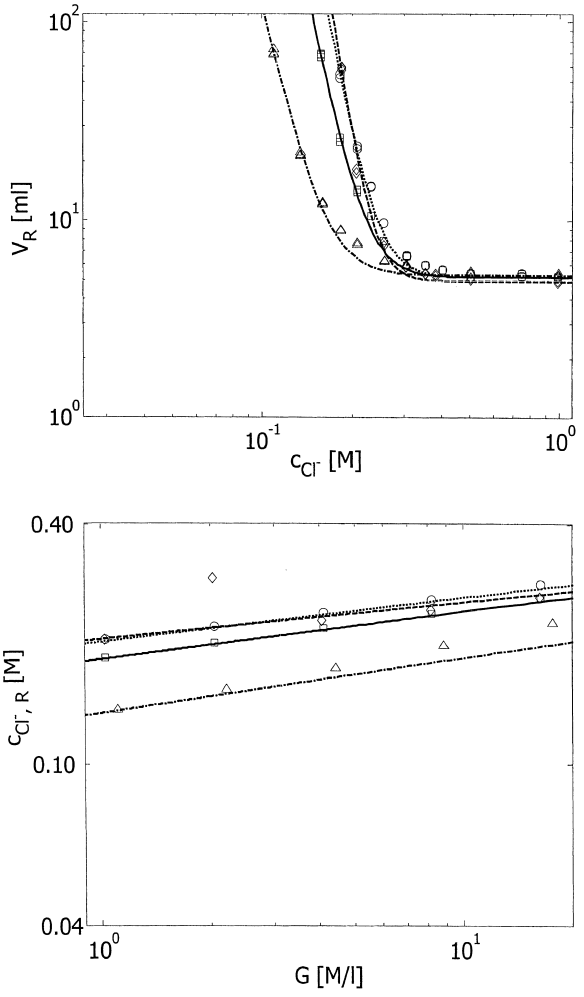


Fig. 2. Whey proteins on Source 30Q at pH 9. Comparison of experimental and correlated isocratic retention volumes (top) and experimental and predicted chloride ion concentrations at gradient elution (bottom). BSA: ◇, exp., - - -, model; α-lactalbumin: △, exp., –·–, model; β-lactoglobulin A: ○, exp., ····, model; β-lactoglobulin B: □, exp., —, model.

gradient elution volume using Eq. (12). The predicted salt concentration at which a protein elutes was calculated from Eq. (14). In some of the gradient elution experiments the protein eluted at the salt concentration $c_{\mathrm{salt}_1}$ after the gradient was finished. This is indicated by a horizontal line. The parameters $\varepsilon_p$, $K_d$, $\Delta G^0_{\mathrm{protein}}$, $\Delta G^0_{\mathrm{counterion}}$, and $\nu$ were all estimated from the isocratic retention data. No parameters were estimated from the gradient elution data, therefore the calculated salt concentrations in the lower graphs are predictions. The results are shown at pH 6 and 9. The results for Source 30Q are shown in Figs. 1 and 2, for Ceramic Q-HyperD F in Figs. 3 and 4, for Merck Fractogel in Figs. 5 and 6, and for Q-Sepharose XL in Figs. 7 and 8. Q-Sepharose XL did not separate β-lactoglobulin A and B. The figures show that the model can correlate the experimental isocratic retention data quite well and that the predicted gradient elution data are in good agreement with the experimental data.

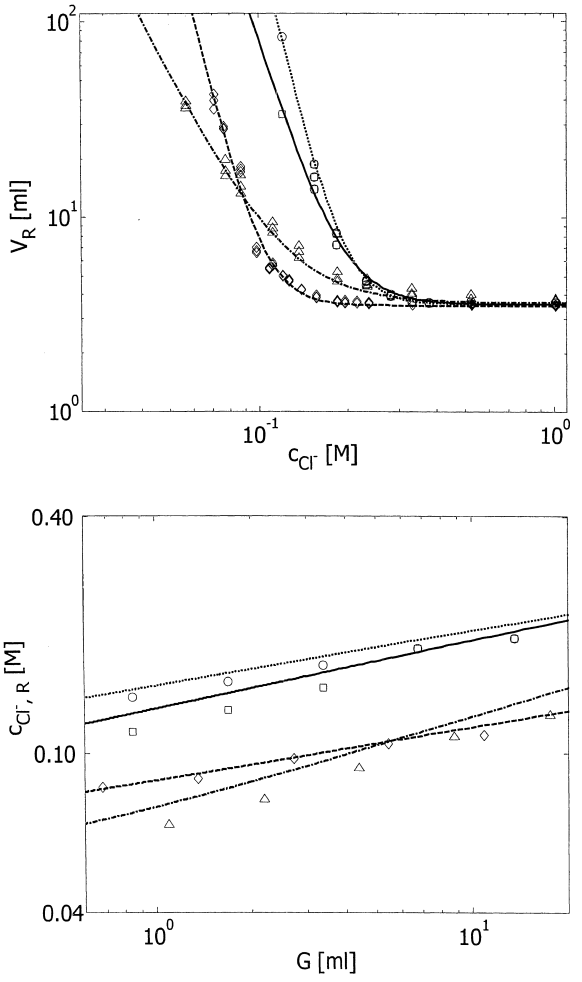


Fig. 3. Whey proteins on Ceramic Q-HyperD F at pH 6. Comparison of experimental and correlated isocratic retention volumes (top) and experimental and predicted chloride ion concentrations at gradient elution (bottom). BSA: ◇, exp., - - -, model; α-lactalbumin: △, exp., –·–, model; β-lactoglobulin A: ○, exp., ···· model; β-lactoglobulin B: □, exp., —, model.

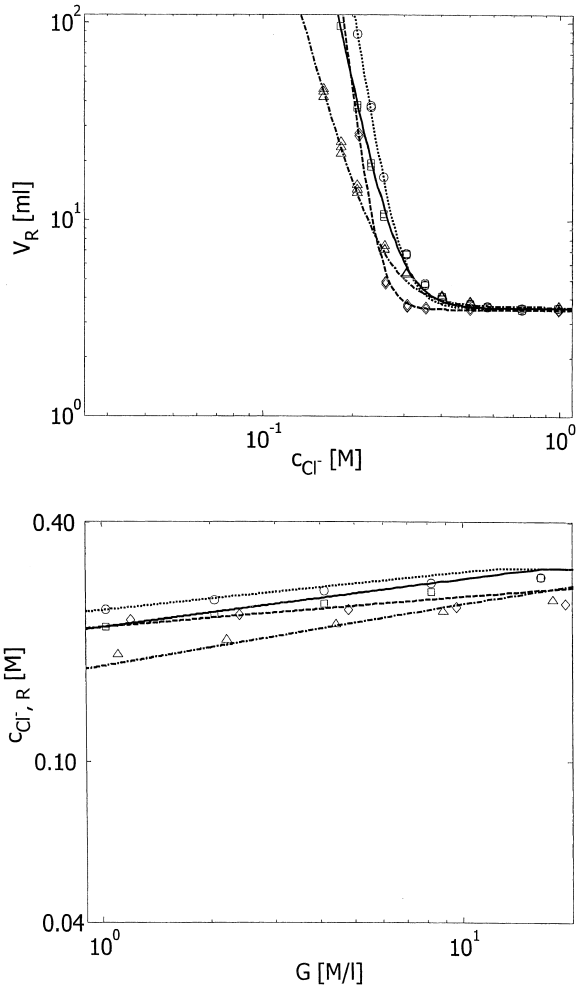


Fig. 4. Whey proteins on Ceramic Q-HyperD F at pH 9. Comparison of experimental and correlated isocratic retention volumes (top) and experimental and predicted chloride ion concentrations at gradient elution (bottom). BSA: ◇, exp., - - -, model; α-lactalbumin: △, exp., –·–, model; β-lactoglobulin A: ○, exp., ····, model; β-lactoglobulin B: □, exp., —, model.

### *3.2. Isocratic elution*

The graphs for the isocratic elution data show that the difference in the retention volumes for the four proteins decrease when pH is increased as one would expect because the isoelectric points are all below 5.5. The data for pH 7 and 8, which are not shown, are in between those at pH 6 and 9. Except for the Source 30Q media, the isocratic elution data at pH 6 show that the elution curve for BSA crosses over the α-lactalbumin elution curve. Furthermore, at pH 6 the data show that the binding strength of β-lactoglobulin A is stronger than the binding strength of β-lactoglobulin B on all media investigated. At pH 9 the elution curves in general become steeper and the

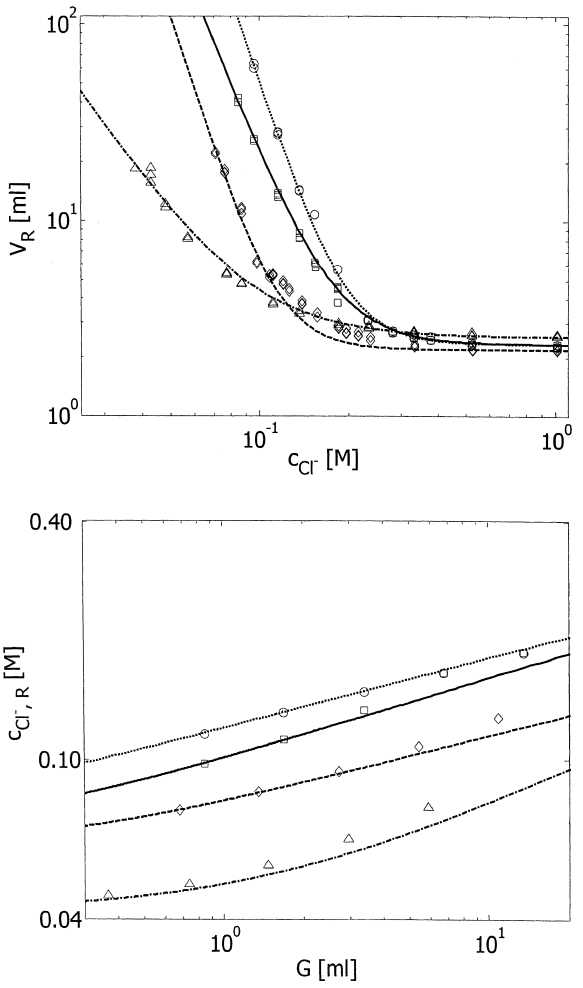


Fig. 5. Whey proteins on Fractogel EMD TMAE 650 (S) at pH 6. Comparison of experimental and correlated isocratic retention volumes (top) and experimental and predicted chloride ion concentrations at gradient elution (bottom). BSA: ◇, exp., - - -, model; α-lactalbumin: △, exp., –·–, model; β-lactoglobulin A: ○, exp., ····, model; β-lactoglobulin B: □, exp., —, model.

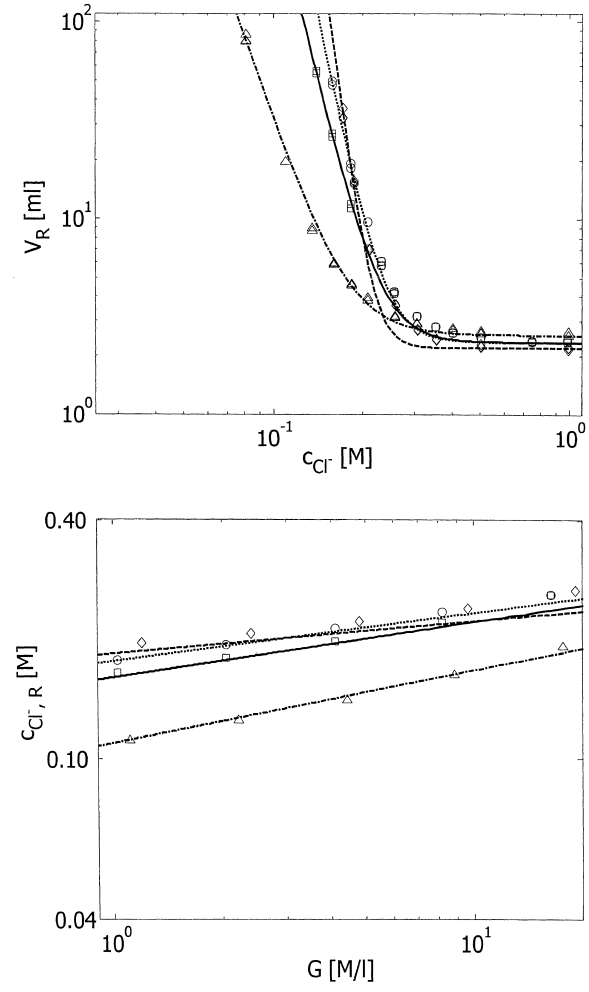


Fig. 6. Whey proteins on Fractogel EMD TMAE 650 (S) at pH 9. Comparison of experimental and correlated isocratic retention volumes (top) and experimental and predicted chloride ion concentrations at gradient elution (bottom). BSA: ◇, exp., - - -, model; α-lactalbumin: △, exp., –·–, model; β-lactoglobulin A: ○, exp., ····, model; β-lactoglobulin B: □, exp., —, model.

elution curve for BSA crosses over all the other elution curves as the salt concentration decreases.

### *3.3. Gradient elution*

The graphs for the gradient elution data show, as one would expect, that the separation becomes more difficult and sometimes impossible when the pH is increased from 6 to 9. On the Source30Q, the Merck Fractogel, and the Q-Sepharose XL media at pH 6 the gradient elution curves are well apart. On the Ceramic Q-HyperD F the elution curves for BSA and α-lactalbumin cross over and similar for the two β-lactoglobulin elution curves. What one should choose as regards media, gradient parameter *G*, and

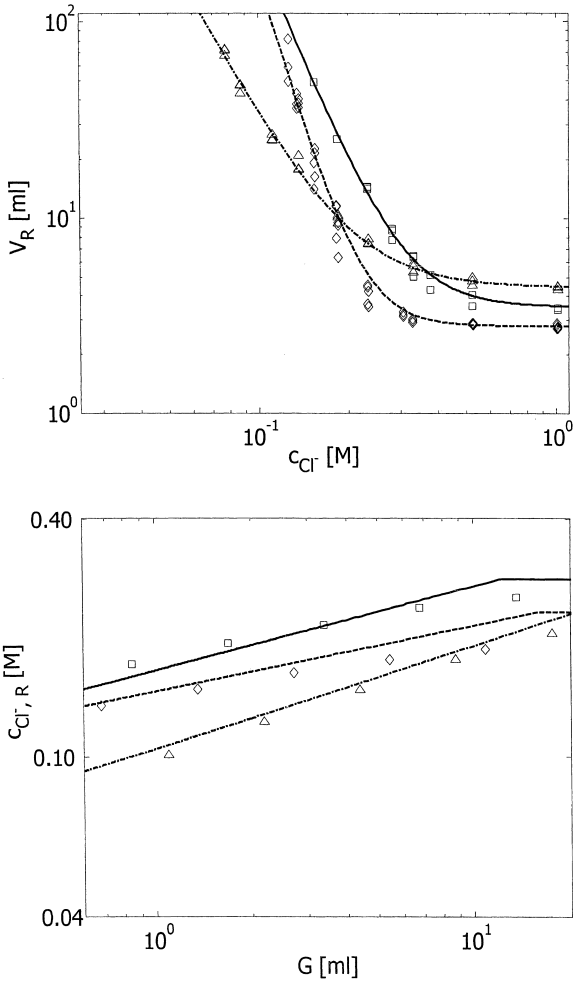


Fig. 7. Whey proteins on Q-Sepharose XL at pH 6. Comparison of experimental and correlated isocratic retention volumes (top) and of experimental and predicted chloride ion concentrations at gradient elution (bottom). BSA: ◇, exp., - - -, model; α-lactalbumin: △, exp., –·–, model; β-lactoglobulin A: ○, exp., ····, model; β-lactoglobulin B: □, exp., —, model.

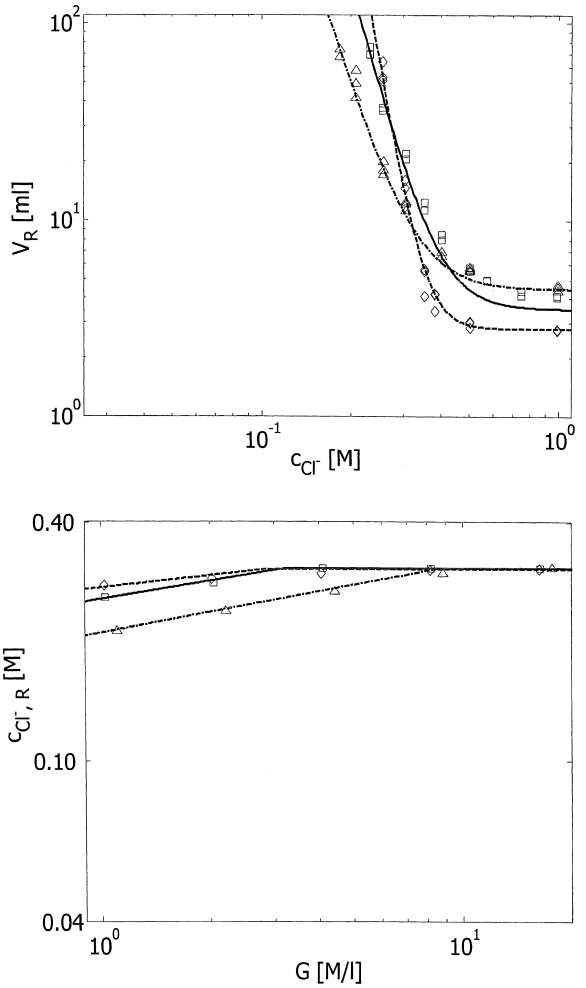


Fig. 8. Whey proteins on Q-Sepharose XL at pH 9. Comparison of experimental and correlated isocratic retention volumes (top) and experimental and predicted chloride ion concentrations at gradient elution (bottom). BSA: ◇, exp., - - -, model; α-lactalbumin: △, exp., –·–, model; β-lactoglobulin A: ○, exp., ····, model; β-lactoglobulin B: □, exp., —, model.

pH cannot be concluded based upon the data presented in this work because it also depends on the mass transfer characteristics which determine the band spreading and thus the resolution.

### *3.4. Estimated model parameters*

The parameters estimated from the isocratic elution volumes for the different media are shown in Tables 3 and 4. We have assessed the bed porosity and calculated the particle porosity from the salt porosity. Nash and Chase [22] used $\varepsilon = 0.4$ and $\varepsilon_p = 0.60–0.65$ for Source 30S and $\varepsilon = 0.35$ and $\varepsilon_p = 0.88$ for SP-Sepharose FF which is similar in structure but not identical to Q-Sepharose XL. Carta and Fernandez [23] have estimated the intraparticle porosity in Q-HyperD F to 0.65. There are no data published for the Merck Fractogel EMD TMAE 650 (S). The estimated standard Gibbs energy changes and the charge ratios $\nu$ are not sensitive to the choice

Table 3
Estimated model parameters for the media

| | Source 30Q | Q-HyperD F Ceramic | Merck Fractogel EMD TMAE 650 (S) | Q Sepharose XL |
|---|---|---|---|---|
| $\varepsilon_t$ salt, $K_d = 1$ | 0.744 | 0.806 | 0.749 | 0.935 |
| $\varepsilon$ | 0.40 | 0.40 | 0.40 | 0.30 |
| $\varepsilon_p$ | 0.57 | 0.68 | 0.58 | 0.91 |
| Equiv./l column volume | 0.105 | 0.316 | 0.029 | 0.285 |
| $\Lambda$ equiv./l pore volume | 0.308 | 0.777 | 0.0825 | 0.448 |
| $\Delta G^0/RT$, $Cl^-$ | 0.320 | −0.322 | 1.457 | 0.363 |

of the particle porosity. If we change $\varepsilon$ by 0.05 units it will not make any visible changes of the results of the correlations, but it will of cause change the numerical values of the parameters slightly. The estimated standard Gibbs energy changes for the salt are positive for all media except the Ceramic Q-

Table 4
Model parameters for four whey proteins on the media Source 30Q, Ceramic Q-HyperD F, Merck Fractogel EMD TMAE 650 (S), and Q-Sepharose XL estimated from the isocratic retention data

| | | BSA | α-Lactalbumin | β-Lactoglobulin A | β-Lactoglobulin B |
|---|---|---|---|---|---|
| Source 30Q | | | | | |
| | $\varepsilon_t$ in 1 *M* salt | 0.611 | 0.654 | 0.641 | 0.641 |
| | $K_d$ | 0.61 | 0.74 | 0.70 | 0.70 |
| | $\Delta G^0/RT$ | 4.663 | 5.049 | 3.444 | 3.718 |
| pH 6 | $\nu$ | 4.20 | 3.64 | 5.04 | 4.29 |
| pH 7 | $\nu$ | 6.16 | 4.74 | 6.21 | 5.50 |
| pH 8 | $\nu$ | 7.89 | 5.33 | 7.21 | 6.56 |
| pH 9 | $\nu$ | 9.77 | 6.31 | 7.96 | 7.31 |
| Ceramic Q-HyperD F | | | | | |
| | $\varepsilon_t$ in 1 *M* salt | 0.467 | 0.482 | 0.474 | 0.474 |
| | $K_d$ | 0.16 | 0.20 | 0.18 | 0.18 |
| | $\Delta G^0/RT$ | 8.224 | 2.713 | 4.507 | 3.090 |
| pH 6 | $\nu$ | 6.05 | 2.94 | 6.11 | 4.63 |
| pH 7 | $\nu$ | 7.78 | 4.11 | 7.61 | 5.84 |
| pH 8 | $\nu$ | 10.44 | 4.77 | 8.57 | 6.57 |
| pH 9 | $\nu$ | 12.29 | 5.50 | 9.60 | 7.28 |
| Merck Fractogel EMD TMAE 650 (S) | | | | | |
| | $\varepsilon_t$ in 1 *M* salt | 0.557 | 0.695 | 0.595 | 0.595 |
| | $K_d$ | 0.45 | 0.85 | 0.56 | 0.56 |
| | $\Delta G^0/RT$ | 4.077 | 2.526 | 1.663 | 1.538 |
| pH 6 | $\nu$ | 4.72 | 2.32 | 4.60 | 3.81 |
| pH 7 | $\nu$ | 6.46 | 3.37 | 6.11 | 5.13 |
| pH 8 | $\nu$ | 8.77 | 3.68 | 6.59 | 5.70 |
| pH 9 | $\nu$ | 11.04 | 4.55 | 7.12 | 6.16 |
| Q-Sepharose XL | | | | β-Lactoglobulin | |
| | $\varepsilon_t$ in 1 *M* salt | 0.371 | 0.590 | 0.465 | |
| | $K_d$ | 0.11 | 0.46 | 0.26 | |
| | $\Delta G^0/RT$ | 3.635 | 2.504 | 1.696 | |
| pH 6 | $\nu$ | 5.01 | 2.76 | 3.69 | |
| pH 7 | $\nu$ | 6.62 | 3.69 | 4.99 | |
| pH 8 | $\nu$ | 8.00 | 4.13 | 5.27 | |
| pH 9 | $\nu$ | 8.83 | 4.74 | 5.55 | |

HyperD F. This may be due to the fact that the Ceramic Q-HyperD F is a more hydrophilic media because the hydrogel filled pores give rise to a high ligand charge density. The Merck Fractogel EMD TMAE 650 (S) has the lowest ligand charge density and thus a more hydrophobic environment and consequently the largest standard Gibbs energy change for the salt. The estimated standard Gibbs energy changes for the proteins reflect a change in the protein conformation upon binding where a stronger binding may bring about a larger conformational change than a weaker binding may cause. But it may also reflect differences in the matrix characteristics like differences in the hydrophobicity. The variations in the standard Gibbs energy changes of the proteins are larger for Ceramic Q-HyperD F than for any of the other media. The difference in the values for the standard Gibbs energy changes of the β-lactoglobulin A and B are −0.27 on Source, 0.13 on Merck Fractogel but 1.5 on Ceramic Q-HyperD which is unexpected when compared to the variations for the other media. The charge ratios for the β-lactoglobulins are larger for A than for B, and the difference is approximately 0.7 on Source, approximately 1 on Merck Fractogel whereas the difference on Q-HyperD varies from 1.5 at pH 6 to 2.3 at pH 9. The standard Gibbs energy change of α-lactalbumin on Q-HyperD is lower than expected when compared with the other media where the standard Gibbs energy change of α-lactalbumin is approximately 1.5 times that of the β-lactoglobulins. The standard Gibbs energy changes on Q-Sepharose XL and on Merck Fractogel are similar and show the same variations for the four proteins whereas on Source the variations are much smaller. The estimated charge ratios increase with increasing pH, and on Q-HyperD they are always larger than for Merck Fractogel, but otherwise there is no apparent trend.

## 4. Conclusion

The results presented in the upper graphs in the figures show that it was possible to correlate the isocratic elution behaviour of four whey proteins in the pH range 6 to 9 on the four anion-exchange media investigated using a simple model, the SMA formalism, because the parameters in the model, the standard Gibbs energy changes and the charge ratio $\nu$, all have a well defined physical significance. The only parameter which depends on the pH is the charge ratio, therefore it is possible to interpolate in the range pH 6–9. Extrapolation is not recommended. The lower graphs in the figures show that, in the gradient elution mode, it is possible to predict the salt concentration at which a protein elutes using the parameters estimated from isocratic elution data alone. The advantage of using the SMA formalism and not an empirical model is that it is straight forward to model the whole isotherm with the SMA formalism and not just the linear range. Eq. (3) is the model for the nonlinear isotherm and by estimating the standard Gibbs energy changes and the charge ratio $\nu$ from the isocratic elution data we have determined two of the parameters in the model. The third parameter is the steric hindrance factor which we estimate from capacity measurements. This shall be the subject of a forthcoming paper.

## Nomenclature

| | |
|---|---|
| $A$ | Distribution ratio $q/c$, initial slope of the isotherm |
| $c$ | Concentration of solute in the mobile phase ($M$) |
| $c_{\mathrm{salt}}$ | Concentration of counter ions in the mobile phase ($M$) |
| $G$ | Gradient parameter in linear gradient elution |
| $G^0$ | Standard state Gibbs energy |
| $K$ | Equilibrium constant in the SMA formalism |
| $K_{\mathrm{d}}$ | Exclusion factor |
| $q$ | Concentration of adsorbed matter in the gel (mol/l pore volume) |
| $q_{\mathrm{salt}}$ | Concentration of counter ions salt at ion-exchanger surface (mol/l pore volume) |
| $R$ | Gas constant (J $\mathrm{mol}^{-1}$ $\mathrm{K}^{-1}$) |
| $V_{\mathrm{column}}$ | Column volume |
| $V_{\mathrm{g}}$ | Gradient volume |
| $V_{\mathrm{NA}}$ | Retention volume of nonadsorbed solute |
| $V_{\mathrm{pore}}$ | Pore volume |
| $V_{\mathrm{R}}$ | Retention volume |
| $z_{\mathrm{s}}$ | Charge of counter ion |
| $z_{\mathrm{p}}$ | Effective charge of protein |

*Greek letters*

| | |
|---|---|
| $\varepsilon_t$ | Total porosity of the column, $\varepsilon + (1 - \varepsilon)\varepsilon_p K_d$ |
| $\varepsilon$ | Interparticle or interstitial porosity, mobile phase volume per column volume |
| $\varepsilon_p$ | Intraparticle porosity, fractional void volume in the particle |
| $\Lambda$ | Capacity of media or charge density (equiv./l pore volume) |
| $\nu$ | Ratio of solute effective charge to counter ion charge |
| $\zeta$ | Steric hindrance factor in the SMA formalism |

## Acknowledgements

The Ceramic Q-HyperD F was a gift from BioSepra and the Source 30Q a gift from Amersham Biotech.

## References

[1] E.N. Lightfoot, Ind. Eng. Chem. Res. 38 (1999) 3628.
[2] R.P. Hahn, M. Schulz, C. Schaupp, A. Jungbauer, J. Chromatogr. A 795 (1998) 277.
[3] E.D. Strange, E.L. Malin, D.L. van Hekken, J.J. Bash, J. Chromatogr. 624 (1992) 81.
[4] P. Konecny, R.J. Brown, W.H. Scouten, J. Chromatogr. A 673 (1994) 45.
[5] S.-C.D. Jen, N. Pinto, Ind. Eng. Chem. Res. 34 (1995) 2685.
[6] C.B. Colby, B.K. O'Neill, F. Vaugham, A.P.J. Middelberg, Biotechnol. Prog. 12 (1996) 662.
[7] S. Vogt, R. Freitag, J. Chromatogr. A 760 (1997) 125.
[8] S.J. Gerberding, C.H. Byers, J. Chromatogr. A 808 (1998) 142.
[9] M.K. Walsh, S.H. Nam, Prep. Biochem. Biotechnol. 31 (2001) 229.
[10] Q. Lan, A. Bassi, J.-X. Zhu, A. Margaritis, Biotechnol. Bioeng. 78 (2002) 157.
[11] C.A. Brooks, S.M. Cramer, AIChE J. 38 (1992) 1969.
[12] J.C. Bosma, J.A. Wesselingh, AIChE J. 44 (1998) 2399.
[13] L. Yonglong, N.G. Pinto, J. Chromatogr. A 702 (1995) 113.
[14] P. Raje, N.G. Pinto, J. Chromatogr. A 760 (1997) 89.
[15] C.M. Roth, A.M. Lenhoff, Langmuir 9 (1993) 962.
[16] C.M. Roth, K.L. Unger, A.M. Lenhoff, J. Chromatogr. A 762 (1996) 45.
[17] G. Guiochon, S.G. Shirazi, A.M. Katti, Academic Press, 1994.
[18] M.D. Le Van, T. Vermeulen, J. Phys. Chem. 85 (1981) 3247.
[19] J.A. Gerstner, J.A. Bell, S.M. Cramer, Biophys. Chem. 52 (1994) 97.
[20] S. Yamamoto, K. Nakanishi, R. Matsuno, Ion-Exchange Chromatography of Proteins, Marcel Dekker, 1988.
[21] Bisgaard-Frantzen, H. Characterization of Column Packings for Chromatograpic Separations of Proteins Ph.D. Dissertation, Technical University of Denmark, 1998.
[22] D.C. Nash, H.A. Chase, J. Chromatogr. A 807 (1998) 185.
[23] G. Carta, M.A. Fernandez, J. Chromatogr. A 746 (1996) 169.